

Interplay between relaxational atomic fluctuations and charge density waves in $\text{La}_{2-x}\text{Sr}_x\text{CuO}_4$ L. Shen^{1,2,3,*}, V. Esposito^{2,3}, N. G. Burdet^{2,3}, M. Zhu⁴, A. N. Petsch⁴, T. P. Croft⁴, S. P. Collins⁵, Z. Ren⁶,
F. Westermeier⁶, M. Sprung⁶, S. M. Hayden^{4,†}, J. J. Turner^{2,3,‡} and E. Blackburn^{1,§}¹*Division of Synchrotron Radiation Research, Department of Physics, Lund University, SE-22100 Lund, Sweden*²*Stanford Institute for Materials and Energy Sciences, Stanford University and SLAC National Accelerator Laboratory, Menlo Park, California 94025, USA*³*Linac Coherent Light Source, SLAC National Accelerator Laboratory, Menlo Park, California 94025, USA*⁴*H.H. Wills Physics Laboratory, University of Bristol, Bristol BS8 1TL, United Kingdom*⁵*Diamond Light Source Ltd., Harwell Science and Innovation Campus, Didcot, Oxfordshire OX11 0DE, United Kingdom*⁶*Deutsches Elektronen-Synchrotron (DESY), Notkestraße 85, 22607 Hamburg, Germany*

(Received 1 April 2022; revised 14 March 2023; accepted 24 October 2023; published 13 November 2023)

In the cuprate superconductors, the spatial coherence of the charge density wave (CDW) state grows below a temperature T_{CDW} , the origin of which is debated. Using x-ray photon correlation spectroscopy, we have studied the temporal atomic relaxation dynamics in $\text{La}_{1.88}\text{Sr}_{0.12}\text{CuO}_4$ to shed light on this question. Cooling within an emergent structurally distorted phase, which favors the CDW modulation in symmetry and develops in two stages between 180 and 120 K, we observe a crossover from cooperativelike to incoherentlike relaxation dynamics at $T_{\text{CDW}} = 75(10)$ K. We argue that, if the CDW is hosted by this distortion, the concomitant relaxational crossover and enhancement of CDW spatial coherence supports the interplay between relaxational atomic fluctuations and CDWs in materials of this class on quasistatic timescales.

DOI: [10.1103/PhysRevB.108.L201111](https://doi.org/10.1103/PhysRevB.108.L201111)

Relaxation and vibration are the two most common forms of atomic dynamics. In the high- T_c Cu-based superconductors, vibration (i.e., phonons) plays a critical role in generating some of the most puzzling physics because its time scale is compatible with those characteristic of electronic processes, leading to, for example, electron-phonon interactions [1]. Relaxation dynamics, on the other hand, are often much slower [2] and therefore appear static on typical electronic time scales. The interplay between relaxation effects and electronic ordering phenomena has rarely been explored in any cuprate.

One ubiquitous electronic order in the cuprates is charge density wave (CDW)—spontaneous modulations of electron density [3]—with a rich, but complicated phenomenology. A well-defined thermodynamic phase transition is missing for the CDWs in most cuprates. Instead, short-range charge correlations can prevail at temperatures far exceeding T_c [4–7]. The widely adopted temperature for characterizing the CDW in the cuprates is T_{CDW} , below which the in-plane correlation length ($\xi_{\text{CDW}}^{\parallel}$) first increases and eventually saturates at a finite value. Since the CDW strongly intertwines with other

electronic degrees of freedom [8], it is important to understand the mechanism defining T_{CDW} .

There is now compelling evidence to show that the CDWs in the cuprates are glasslike [9,10] and fluctuate on exceptionally slow timescales (10^{-1} s - 10^4 s) [11–15]. Consequently, relaxation effects, which occur on similar time scales and are another inherent property in these materials due to their defective atomic lattice introduced by carrier doping [16–18], are no longer negligible. Fundamental to this is the question: Can these slow temporal fluctuations of atoms offer information on the formation of the more spatially coherent CDW state at T_{CDW} ?

To address this question, we have measured the atomic relaxation dynamics in $\text{La}_{1.88}\text{Sr}_{0.12}\text{CuO}_4$ using x-ray photon correlation spectroscopy (XPCS). This technique relies on the configurational change of speckle patterns [Fig. 1(a)]—complex scattering images generated by the interference between the coherent x-rays and local structure—in the time (t) domain to calculate the intermediate scattering function $|F(\mathbf{Q}, t)|$ at a momentum transfer \mathbf{Q} [19,20]. In general, atomic relaxation can be directly probed by the speckles near a Bragg reflection [21–23]. Accordingly, we have collected a time series of x-ray diffuse scattering (XDS) patterns near the $\mathbf{Q}_0 = (0, 0, 4)$ reflection in $\text{La}_{1.88}\text{Sr}_{0.12}\text{CuO}_4$ [Fig. 1(b)]. \mathbf{Q}_0 is indexed in the high-temperature tetragonal (HTT, space group $I4/mmm$) notation, and so are the other reflections studied in this work. \mathbf{Q}_0 is specular, chosen specifically to minimize the XDS contamination from the low-temperature orthorhombic (LTO, space group $Bmab$) twinning in the ab plane [24], which is induced by the HTT-LTO structural phase transition at $T_{\text{LTO}} = 240$ K (Supplemental Material) [25]; \mathbf{Q}_0 is also the most intense Bragg reflection accessible in our scattering geometry

*lingjia.shen@sljus.lu.se

†S.Hayden@bristol.ac.uk

‡joshuat@slac.stanford.edu

§elizabeth.blackburn@sljus.lu.se

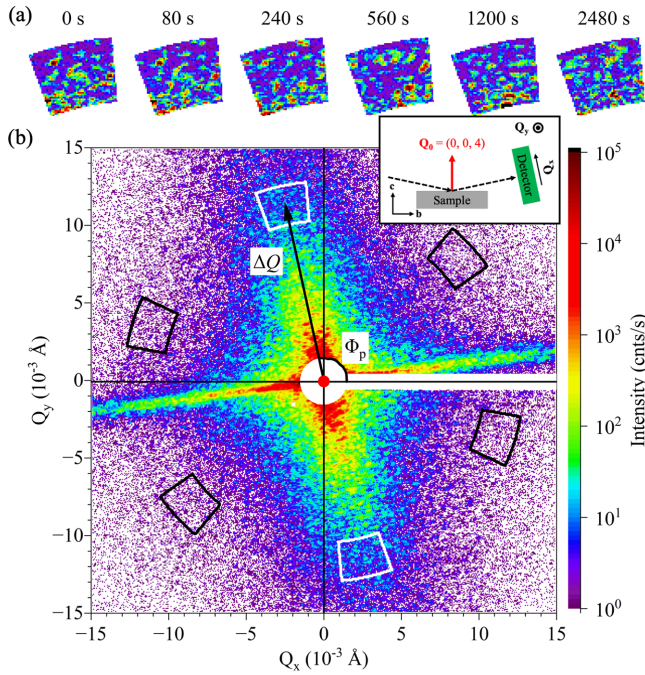


FIG. 1. Coherent XDS near $\mathbf{Q}_0 = (0, 0, 4)$ at 30 K. (a) Temporal evolution of the speckles in the top white box below. (b) Single-frame XDS profile. A polar coordinate convention centered at \mathbf{Q}_0 (red dot) is defined. White and black boxes are on- and off- axis ensembles (main text). The sharp streak is a CTR. Inset: Top view of the experimental geometry.

[inset, Fig. 1(b)]. The detailed data collection and analysis protocols for extracting $|F(\mathbf{Q}, t)|$ are described in the Supplemental Material [25]. In addition, a polar coordinate system centered at \mathbf{Q}_0 is used to map out the relative momentum transfer $\Delta\mathbf{Q}(\Delta Q, \Phi) = \mathbf{Q} - \mathbf{Q}_0$ in the detector plane [Fig. 1(b)]. At all temperatures, we observe a sharp crystal truncation rod (CTR) traversing \mathbf{Q}_0 at $\Phi_{\text{CTR}} \simeq 7.5^\circ/187.5^\circ$.

Two $\text{La}_{1.88}\text{Sr}_{0.12}\text{CuO}_4$ single crystals were used for this work; they were cut from the same batch as the one studied in Ref. [4], which reported $T_{\text{CDW}} = 75(10)$ K. These samples were grown by the traveling-solvent floating-zone method described in Ref. [26], and then mechanically cleaved on one side to expose a natural facet with the c axis normal. The hard x-ray diffraction (HXD) experiment was performed on the I16 beamline at the Diamond Light Source (United Kingdom), using a monochromatic x-ray beam with energy 8.095 keV. The XDS and XPCS experiment was carried out at the coherent x-ray scattering beamline P10 of the PETRA III storage ring (Germany). A monochromatic x-ray beam (energy 8.5 keV) was focused at the sample position with spot size of $2.5 \times 2.5 \mu\text{m}^2$ in full width at half maximum. Both experiments were performed in the $\theta/2\theta$ reflection geometry [inset, Fig. 1(b)].

The XDS profile at 30 K has a profound anisotropy along $\Phi = \Phi_p \simeq 102.5^\circ/282.5^\circ$ [Fig. 1(b)]. This anisotropy axis is insensitive to heating up to $T_{\text{D1}} = 180$ K, above which the profile becomes almost isotropic in Φ [Fig. 4(a)]; we will revisit T_{D1} in detail below. It is convenient to define two types of \mathbf{Q} ensembles for studying the $|F(\mathbf{Q}, t)|$ at $T < T_{\text{D1}}$: The on-axis ensemble centered at Φ_p , and the off-axis ensemble centered

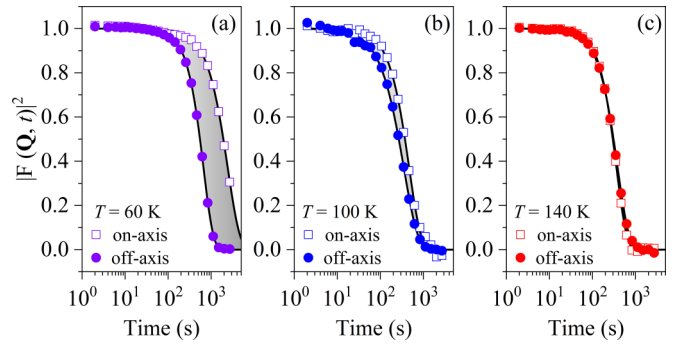


FIG. 2. Intermediate scattering function $|F(\mathbf{Q}, t)|$. On- (open squares) and off- (filled circles) axis $|F(\mathbf{Q}, t)|^2$ curves at (a) 60 K, (b) 100 K, and (c) 140 K. Solid lines are the single-KWW fits (main text). A strong anisotropy in the relaxation develops between 100 K and 60 K, while the x-ray diffuse scattering only evolves smoothly in this temperature window [Fig. 4(a)].

at $\Phi_p \pm 60^\circ$ (chosen to access the scattering away from Φ_p while avoiding the CTR contamination). For speckle sampling purposes (Supplemental Material [25]), these ensembles have finite radial and azimuthal coverages of $\pm 0.13 \times 10^{-2} \text{\AA}^{-1}$ and $\pm 7.5^\circ$, respectively [Fig. 1(b)]. We have computed the $|F(\mathbf{Q}, t)|$ in the on- and off- axis ensembles as a function of ΔQ . The major finding of this report—interplay between the atomic relaxation and CDW—is present at all ΔQ values. For simplicity, we will only discuss the data in the on- and off-axis ensembles at $\Delta Q = 1.16 \times 10^{-2} \text{\AA}^{-1}$.

We focus on the relaxation dynamics below T_{D1} , which we show later is relevant for the CDW in $\text{La}_{1.88}\text{Sr}_{0.12}\text{CuO}_4$, while those at higher temperatures are presented in Supplemental Material [25]. As shown in Fig. 2, the $|F(\mathbf{Q}, t)|$ data can be well reproduced by the Kohlrausch-Williams-Watts (KWW) decay model:

$$|F(\mathbf{Q}, t)| = \exp[-(\Gamma t)^\beta]. \quad (1)$$

In this equation, Γ and β are the relaxation rate and exponent of the decay process, respectively. The decay shape parameter β is an indicator for the nature of the dynamics [19,20]. In $\text{La}_{1.88}\text{Sr}_{0.12}\text{CuO}_4$, β is always between 1.0 and 2.0 for both on- and off- axis dynamics [inset, Fig. 3(a)]. Such compressed decay is commonly observed in glassy systems [19,20,22,23,27].

A visual inspection on $|F(\mathbf{Q}, t)|^2$ (Fig. 2) reveals a strong anisotropy at 60 K. It is much weaker at 100 K, and becomes barely resolvable at 140 K. To precisely capture this temperature-induced change in relaxation anisotropy, we study the on- (Γ_{on}) and off- (Γ_{off}) axis relaxation rates. These two parameters are plotted in Fig. 3(a). Above 120 K, which we label T_{D2} hereinafter, Γ_{on} and Γ_{off} have small differences; but they show no systematic trend as the temperature decreases. Upon further cooling, Γ_{on} becomes smaller than Γ_{off} at T_{D2} ; this holds for the atomic relaxation in the entire ΔQ window probed. Interestingly, the $\Gamma_{\text{on}} < \Gamma_{\text{off}}$ feature gets sharply enhanced in the 85–70 K window. This enhancement can be quantitatively characterized by the unitless relaxation anisotropy parameter $K_\Gamma = \frac{\Gamma_{\text{on}} - \Gamma_{\text{off}}}{\Gamma_{\text{on}} + \Gamma_{\text{off}}}$ [Fig. 3(b)]. Above 85 K, K_Γ varies in a narrow range between about 45 0.10 and 0.05.

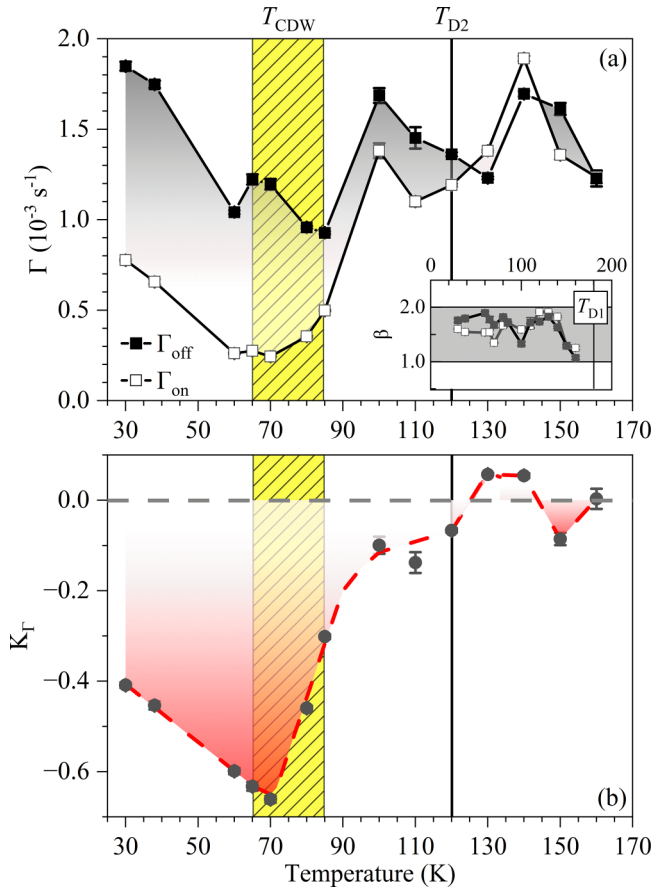


FIG. 3. Atomic relaxation anisotropy. (a) On- (open squares) and off- (filled squares) axis KWW relaxation rate Γ (main panel) and exponent β (inset). (b) relaxation anisotropy parameter (main text) as a function of temperature. Dashed lines are guides for the eye.

While K_{Γ} has a smoothly decreasing tendency (at best) between T_{D2} and 85 K, a much more dramatic reduction occurs around $T_{\text{CDW}} = 75(10)$ K [4,5]: It changes from about -0.3 at 85 K to -0.63 at 70 K. A kink is seen at 70 K, below which K_{Γ} increases almost linearly and eventually reaches about -0.40 at 30 K.

Within the errors, the temperature window where K_{Γ} sharply drops agrees with $T_{\text{CDW}} = 75(10)$ K [Fig. 3(b)], which was obtained from a crystal cut from the same batch as ours [4]. In the following, we elucidate the correlation between the atomic relaxation dynamics and CDWs in $\text{La}_{1.88}\text{Sr}_{0.12}\text{CuO}_4$. This is done in two steps. In the first step, we quantitatively study the anisotropic XDS profile that generates the speckles used for extracting $|F(\mathbf{Q}, t)|$ below T_{D1} [Fig. 1(b)]. In the second step, we show evidence revealing the origin of this anisotropic scattering—an emergent symmetry-breaking distortion that favors the CDW modulation.

We start with the pixel-averaged on- and off- axis XDS amplitudes ($I_{\text{on}}/I_{\text{off}}$) in the same ensembles used for the XPCS analysis [Fig. 1(b)]. As shown in Fig. 4(a), I_{on} and I_{off} are small and almost identical during the initial cooling from 200 K, supporting that the XDS profile is quasi-isotropic. A large XDS signal develops in both channels at T_{D1} , accompanied by the development of the Φ_p anisotropy that prevails at lower temperatures. I_{off} is re-entrantly suppressed at T_{D2} ,

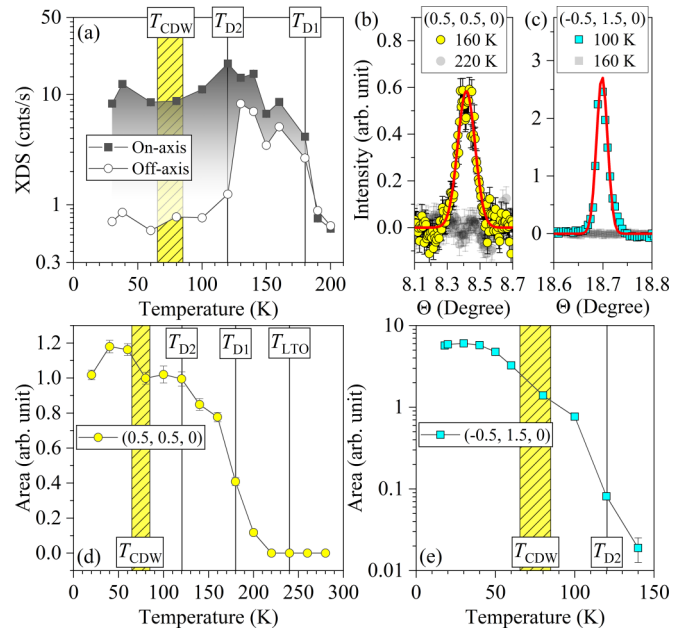


FIG. 4. Local and global atomic configurations. (a) On- and off- axis XDS amplitudes vs temperature. (b) and (c) LTO/HTT-forbidden reflections. Red lines are Gaussian fits. (d) and (e) Areas of the two LTO/HTT-forbidden reflections as a function of temperature. Temperatures marked in (a) (d), and (e) are defined in the main text.

making the XDS even more anisotropic. No XDS anomaly can be unambiguously resolved at T_{CDW} .

In theory, XDS can be directly linked to the local atomic configuration [28]. The temperature dependences of the XDS amplitudes [Fig. 4(a)] reveal a complex local reconstruction process of atoms in $\text{La}_{1.88}\text{Sr}_{0.12}\text{CuO}_4$, which starts at T_{D1} and completes at T_{D2} . This can be caused by a structural phase transition. Since these changes occur well below $T_{\text{LTO}} = 240$ K (Supplemental Material [25]), they are not associated with the LTO distortion. Previously, a symmetry-breaking, monoclinic-like structural distortion (space group $P2/m$), which favors the CDW modulation based on a group theory analysis, has been reported in the LTO phase of $\text{La}_{1.88}\text{Sr}_{0.12}\text{CuO}_4$ [29]. Using synchrotron HXD, we have tracked the evolution of this emergent phase as a function of temperature, which can be uniquely characterized by the reflections that are forbidden in both HTT and LTO space groups, e.g., $(0.5, 0.5, 0)$ and $(-0.5, 1.5, 0)$. Notably, we find that these reflections, which can be indexed by the space group $P2/m$ [29], have different characteristic temperatures [Figs. 4(b) and 4(c)].

We fit their profiles to a Gaussian function. The peak at $(0.5, 0.5, 0)$ is about five times broader than that at $(-0.5, 1.5, 0)$. This broadening is primarily due to the in-plane twinning induced by the LTO distortion [30]. After taking into account the resolution effect, we estimate the coherence length defining the $Bmab$ -symmetry-breaking distortions to be at least 400 \AA ; this is consistent with that reported previously [29]. In Figs. 4(d) and 4(e), we study the temperature dependences of these reflections. The $(0.5, 0.5, 0)$ reflection becomes finite at 200 K (i.e., 40 K below T_{LTO}) and then increases dramatically at $T_{\text{D1}} = 180$ K [Fig. 4(d)]. On the

other hand, the $(-0.5, 1.5, 0)$ reflection does not become resolvable until 140 K, before it sharply rises below $T_{D2} = 120$ K [Fig. 4(e)]. Combining the HXD and XDS results, we suggest that there is a symmetry-breaking, monocliniclike distortion inside the LTO phase. This distortion develops in two stages; they are responsible for the reconstructions of XDS profile at T_{D1} and T_{D2} . As a result, the speckles generated by the anisotropic XDS and used for relaxation dynamics analysis below T_{D1} are correlated with this distortion, which has been proposed to favor the CDW modulation in symmetry [29].

Having established a strong connection between the atomic relaxation dynamics and CDWs in $\text{La}_{1.88}\text{Sr}_{0.12}\text{CuO}_4$ via a combined XDS and HXD study, we now come back to discuss the relaxation anisotropy, and more importantly, its interplay with the CDW spatial coherence. In general, atoms can relax either incoherently or cooperatively. In an incoherent process, the dynamics are governed by the local atomic configuration, because the atoms are in the non-interacting limit. Accordingly, the KWW relaxation rate Γ [Eq. (1)] is a monotonically decreasing function of the XDS amplitude [31,32]. This phenomenon is called de Gennes (dG) narrowing, and has been observed in diluted glasses [21].

The dG narrowing model would require, (1) $\Gamma_{\text{on}} < \Gamma_{\text{off}}$ ($K_{\Gamma} < 0$) below T_{D1} , where $I_{\text{on}} > I_{\text{off}}$, (2) a further decrease of K_{Γ} when the temperature is lowered across T_{D2} , where the enhancement in XDS anisotropy is most dramatic, and (3) no significant change in K_{Γ} at T_{CDW} , where the XDS evolves smoothly [Fig. 4(a)]. However, as shown in Fig. 3(b), the sign of K_{Γ} fluctuates randomly between T_{D1} and T_{D2} ; the biggest reduction in K_{Γ} occurs at T_{CDW} instead of T_{D2} . The loose coupling between the relaxation rate and XDS amplitude at these temperatures does not fit this prediction. Instead, it is strong evidence for cooperativelike relaxation [27]. Typically, cooperative dynamics are driven by interatomic interactions. In theory, they can be stabilized by nonlocal (overlapping) strain fields [33,34]. The strain field in the La-based cuprates comes from the Sr dopants [28]. Its correlation length can be estimated by $2\pi/|\Delta Q|$. As shown in Fig. 1(b), the XDS intensity drops by at least two orders of magnitude within a $|\Delta Q|$ range of 0.015 \AA^{-1} , corresponding to a strain field that extends about 500 \AA in space. This can lead to the cooperativelike relaxation observed. Although K_{Γ} is weakly suppressed at T_{D2} , a considerable reduction is observed inside the T_{CDW} window. This supports the idea that the dG narrowing picture, i.e., incoherent-like atomic relaxation dynamics, is recovered below T_{CDW} . In other words, there is a crossover from cooperative- to incoherentlike atomic relaxation dynamics when the sample is cooled below T_{CDW} .

Previously, the variation in CDW spatial coherence $\xi_{\text{CDW}}^{\parallel}$ in the cuprates has been understood in the context of static disorder [10,18,35], or intertwining with superconductivity [6,36]. In $\text{La}_{1.88}\text{Sr}_{0.12}\text{CuO}_4$, we observe that a new structural distortion, which favors the CDW in symmetry [29], develops in the normal state and well above T_{CDW} [Figs. 4(d) and 4(e)]. But a longer $\xi_{\text{CDW}}^{\parallel}$ does not immediately follow at T_{D1} or T_{D2} [4,5]. If this emergent distortion hosts the CDWs observed in $\text{La}_{1.88}\text{Sr}_{0.12}\text{CuO}_4$ [4,5], other factors need to be considered.

The crossover in temporal relaxation dynamics of atoms around T_{CDW} can offer important insights into this puzzle.

While the CDW modulation in $\text{La}_{1.88}\text{Sr}_{0.12}\text{CuO}_4$ is compatible with the distortion observed by HXD in symmetry [29], the Sr dopants generate strain fields that can drive the surrounding atoms away from their ideal positions defined by the otherwise clean crystal structure [28]. These atoms then spontaneously relax in space-dynamics probed in our XPCS measurements. By definition, atoms wiggle around their ideal positions in the incoherent relaxation limit. In the cooperative relaxation limit, on the other hand, the time-averaged wiggling centers are decoupled from these ideal positions due to the interatomic interactions imposed by the nonlocal strain fields [33,34]. The ideal positions, which arise from the symmetry-breaking, monocliniclike distortion [Figs. 4(b)–4(e)], favor the CDW modulation [29]. This means that, at any given time, $\xi_{\text{CDW}}^{\parallel}$ depends on the number of clustering atoms that can be found at these positions. Accordingly, the CDW state is relatively more spatially coherent when the atoms are undergoing the incoherent-like relaxation process. This provides a different scenario to explain the enhanced $\xi_{\text{CDW}}^{\parallel}$ below T_{CDW} , in addition to the ones involving static disorder [10,18,35] or electronic intertwining [6,36]. Finally, we stress that the temporal fluctuations, given by the two distinct types of atomic relaxation described above lead to identical diffraction patterns in traditional XDS measurements; they can only be distinguished through the temporal autocorrelations observed through speckle analysis enabled by coherent x-ray scattering, e.g., XPCS.

The two-stage development of the emergent atomic distortion characterized by the LTO/HTT-forbidden reflections, together with the concomitant emergence of an anisotropic XDS profile, are puzzling [Figs. 1(b) and 4]. For example, these reflections are also forbidden in the so-called low-temperature tetragonal (LTT) notation (space group $P4_2/nm$), where the associated CuO_6 octahedral rotation stabilizes the CDW state in $\text{La}_{2-x}\text{Ba}_x\text{CuO}_4$ [37] and $\text{La}_{1.8-x}\text{Eu}_{0.2}\text{Sr}_x\text{CuO}_4$ [7] at low temperatures. However, the CDW correlations in these materials can persist at high temperatures where the LTT distortion is suppressed and weak monocliniclike distortions are present [38]. As a result, our results, which focus on the CDWs outside the LTT phase, are not incompatible with previous studies. Since this emergent distortion is important for understanding the CDW modulations [29], more studies on the global and local atomic configurations underlying these changes are needed.

Although it is broadly acknowledged that the CDWs in the cuprate superconductors are glasslike [9,10,35], exhibit quasistatic fluctuations [11–15], and can couple to the atomic lattice on different length scales [10,39], no existing theory or experiment has accounted for their coupling to atomic relaxation dynamics which have compatible quasistatic time scales. Using XPCS, we show that the CDW spatial coherence $\xi_{\text{CDW}}^{\parallel}$ in $\text{La}_{1.88}\text{Sr}_{0.12}\text{CuO}_4$ gets enhanced—not at the temperature where a distortion that favors the CDW modulation emerges (T_{D1}/T_{D2})—but at a temperature where the atomic relaxation dynamics undergo a cooperative-to-incoherent crossover (T_{CDW}). We show that the interplay between these relaxational atomic fluctuations and CDWs can lead to the enhanced $\xi_{\text{CDW}}^{\parallel}$ below T_{CDW} . Since almost all cuprate superconductors are intrinsically disordered, and more importantly, possess a significant amount of dopants that

can induce nonlocal strain fields, the importance of atomic relaxation dynamics for understanding the CDW state, especially $\xi_{\text{CDW}}^{\parallel}$, goes beyond the La-based family. As a result, our work calls for further studies on the many-body interactions in the so far largely unexplored quasielastic time regime.

The authors thank M. Senn and A. Bombardi for fruitful discussions. LS and EB's work is supported in part by

Crafoordska stiftelsen (reference number 20190930). This work is also supported by the U.S. Department of Energy, Office of Science, Basic Energy Sciences, Materials Sciences and Engineering Division, under Contract No. DE-AC02-76SF00515. J.J.T. acknowledges support from the U.S. DOE, Office of Science, Basic Energy Sciences through the Early Career Research Program. We acknowledge Diamond Light Source for time on Beamline I16 under Proposal MT11098.

-
- [1] T. Cuk, D. H. Lu, X. J. Zhou, Z.-X. Shen, T. P. Devereaux, and N. Nagaosa, A review of electron-phonon coupling seen in the high-Tc superconductors by angle-resolved photoemission studies (ARPES), *Physica Status Solidi (b)* **242**, 11 (2005).
- [2] J. C. Qiao and J. M. Pelletier, Dynamic mechanical relaxation in bulk metallic glasses: A review, *J. Mater. Sci. Technol.* **30**, 523 (2014).
- [3] R. Comin and A. Damascelli, Resonant x-ray scattering studies of charge order in cuprates, *Annu. Rev. Condens. Matter Phys.* **7**, 369 (2016).
- [4] T. P. Croft, C. Lester, M. S. Senn, A. Bombardi, and S. M. Hayden, Charge density wave fluctuations in $\text{La}_{2-x}\text{Sr}_x\text{CuO}_4$ and their competition with superconductivity, *Phys. Rev. B* **89**, 224513 (2014).
- [5] H. Miao, G. Fabbris, R. J. Koch, D. G. Mazzone, C. S. Nelson, R. Acevedo-Esteves, G. D. Gu, Y. Li, T. Yilmaz, K. Kaznatcheev, E. Vescovo, M. Oda, T. Kurosawa, N. Momono, T. Assefa, I. K. Robinson, E. S. Bozin, J. M. Tranquada, P. D. Johnson, and M. P. M. Dean, Charge density waves in cuprate superconductors beyond the critical doping, *npj Quantum Mater.* **6**, 31 (2021).
- [6] R. Arpaia, S. Caprara, R. Fumagalli, G. De Vecchi, Y. Y. Peng, E. Andersson, D. Betto, G. M. De Luca, N. B. Brookes, F. Lombardi, M. Salluzzo, L. Braicovich, C. Di Castro, M. Grilli, and G. Ghiringhelli, Dynamical charge density fluctuations pervading the phase diagram of a Cu-based high-Tc superconductor, *Science* **365**, 906 (2019).
- [7] Q. Wang, M. Horio, K. von Arx, Y. Shen, D. John Mukkattukavil, Y. Sassa, O. Ivashko, C. E. Matt, S. Pyon, T. Takayama, H. Takagi, T. Kurosawa, N. Momono, M. Oda, T. Adachi, S. M. Haidar, Y. Koike, Y. Tseng, W. Zhang, J. Zhao *et al.*, High-temperature charge-stripe correlations in $\text{La}_{1.675}\text{Eu}_{0.2}\text{Sr}_{0.125}\text{CuO}_4$, *Phys. Rev. Lett.* **124**, 187002 (2020).
- [8] B. Keimer, S. A. Kivelson, M. R. Norman, S. Uchida, and J. Zaanen, From quantum matter to high-temperature superconductivity in copper oxides, *Nature (London)* **518**, 179 (2015).
- [9] M. Vojta, Lattice symmetry breaking in cuprate superconductors: stripes, nematics, and superconductivity, *Adv. Phys.* **58**, 699 (2009).
- [10] L. Nie, G. Tarjus, and S. A. Kivelson, Quenched disorder and vestigial nematicity in the pseudogap regime of the cuprates, *Proc. Natl. Acad. Sci. USA* **111**, 7980 (2014).
- [11] X. M. Chen, V. Thampy, C. Mazzoli, A. M. Barbour, H. Miao, G. D. Gu, Y. Cao, J. M. Tranquada, M. P. M. Dean, and S. B. Wilkins, Remarkable stability of charge density wave order in $\text{La}_{1.875}\text{Ba}_{0.125}\text{CuO}_4$, *Phys. Rev. Lett.* **117**, 167001 (2016).
- [12] V. F. Mitrović, M.-H. Julien, C. de Vaulx, M. Horvatić, C. Berthier, T. Suzuki, and K. Yamada, Similar glassy features in the ^{139}La NMR response of pure and disordered $\text{La}_{1.88}\text{Sr}_{0.12}\text{CuO}_4$, *Phys. Rev. B* **78**, 014504 (2008).
- [13] I. Raičević, J. Jaroszyński, D. Popović, C. Panagopoulos, and T. Sasagawa, Evidence for charge glasslike behavior in lightly doped $\text{La}_{2-x}\text{Sr}_x\text{CuO}_4$ at low temperatures, *Phys. Rev. Lett.* **101**, 177004 (2008).
- [14] D. S. Caplan, V. Orlyanchik, M. B. Weissman, D. J. Van Harlingen, E. H. Fradkin, M. J. Hinton, and T. R. Lemberger, Anomalous noise in the pseudogap regime of $\text{YBa}_2\text{Cu}_3\text{O}_{7-\delta}$, *Phys. Rev. Lett.* **104**, 177001 (2010).
- [15] P. G. Baity, T. Sasagawa, and D. Popović, Collective dynamics and strong pinning near the onset of charge order in $\text{La}_{1.48}\text{Nd}_{0.4}\text{Sr}_{0.12}\text{CuO}_4$, *Phys. Rev. Lett.* **120**, 156602 (2018).
- [16] I. Martin and A. V. Balatsky, Doping-induced inhomogeneity in high-Tc superconductors, *Physica C* **357-360**, 46 (2001).
- [17] I. Zeljkovic, Z. Xu, J. Wen, G. Gu, R. S. Markiewicz, and J. E. Hoffman, Imaging the impact of single oxygen atoms on superconducting $\text{Bi}_{2+y}\text{Sr}_{2-y}\text{CaCu}_2\text{O}_{8+x}$, *Science* **337**, 320 (2012).
- [18] G. Campi, A. Bianconi, N. Poccia, G. Bianconi, L. Barba, G. Arrighetti, D. Innocenti, J. Karpinski, N. D. Zhigadlo, S. M. Kazakov, M. Burghammer, M. v. Zimmermann, M. Sprung, and A. Ricci, Inhomogeneity of charge-density-wave order and quenched disorder in a high-tc superconductor, *Nature (London)* **525**, 359 (2015).
- [19] A. Madsen, R. L. Leheny, H. Guo, M. Sprung, and O. Czakkel, Beyond simple exponential correlation functions and equilibrium dynamics in x-ray photon correlation spectroscopy, *New J. Phys.* **12**, 055001 (2010).
- [20] S. K. Sinha, Z. Jiang, and L. B. Lurio, X-ray photon correlation spectroscopy studies of surfaces and thin films, *Adv. Mater.* **26**, 7764 (2014).
- [21] M. Leitner, B. Sepiol, L.-M. Stadler, B. Pfau, and G. Vogl, Atomic diffusion studied with coherent x-rays, *Nat. Mater.* **8**, 717 (2009).
- [22] B. Ruta, Y. Chushkin, G. Monaco, L. Cipelletti, E. Pineda, P. Bruna, V. M. Giordano, and M. Gonzalez-Silveira, Atomic-scale relaxation dynamics and aging in a metallic glass probed by x-ray photon correlation spectroscopy, *Phys. Rev. Lett.* **109**, 165701 (2012).
- [23] V. M. Giordano and B. Ruta, Unveiling the structural arrangements responsible for the atomic dynamics in metallic glasses during physical aging, *Nat. Commun.* **7**, 10344 (2016).
- [24] X. Y. Zheng, R. Feng, D. S. Ellis, and Y.-J. Kim, Bulk-sensitive imaging of twin domains in $\text{La}_{2-x}\text{Sr}_x\text{CuO}_4$ under uniaxial pressure, *Appl. Phys. Lett.* **113**, 071906 (2018).
- [25] See Supplemental Materials at <http://link.aps.org/supplemental/10.1103/PhysRevB.108.L201111> for the HTT-LTO transition,

- XPCS data analysis process, and atomic relaxation dynamics at $T \geq_{D1} = 180$ K, which also includes Refs. [40–42].
- [26] S. Komiya, Y. Ando, X. F. Sun, and A. N. Lavrov, *c*-axis transport and resistivity anisotropy of lightly to moderately doped $\text{La}_{2-x}\text{Sr}_x\text{CuO}_4$ single crystals: Implications on the charge transport mechanism, *Phys. Rev. B* **65**, 214535 (2002).
- [27] C. Caronna, Y. Chushkin, A. Madsen, and A. Cupane, Dynamics of nanoparticles in a supercooled liquid, *Phys. Rev. Lett.* **100**, 055702 (2008).
- [28] J. Q. Lin, X. Liu, E. Blackburn, S. Wakimoto, H. Ding, Z. Islam, and S. K. Sinha, Quantitative characterization of the nanoscale local lattice strain induced by Sr dopants in $\text{La}_{1.92}\text{Sr}_{0.08}\text{CuO}_4$, *Phys. Rev. Lett.* **120**, 197001 (2018).
- [29] R. Frison, J. K uspert, Q. Wang, O. Ivashko, M. v. Zimmermann, M. Meven, D. Bucher, J. Larsen, C. Niedermayer, M. Janoschek, T. Kurosawa, N. Momono, M. Oda, N. B. Christensen, and J. Chang, Crystal symmetry of stripe-ordered $\text{La}_{1.88}\text{Sr}_{0.12}\text{CuO}_4$, *Phys. Rev. B* **105**, 224113 (2022).
- [30] Two types of orthogonal twin domains exist below T_{LTO} [43]; this is observed in our HXD measurements too. The *Bmab*-forbidden reflection (0.5, -0.5, 0) scattered by the twin domains, which lies $0.05(1)^\circ$ away from (0.5, 0.5, 0) in Θ , causes the peak broadening in Fig. 1(a).
- [31] P. De Gennes, Liquid dynamics and inelastic scattering of neutrons, *Physica* **25**, 825 (1959).
- [32] S. Sinha and D. Ross, Self-consistent density response function method for dynamics of light interstitials in crystals, *Physica B+C* **149**, 51 (1988).
- [33] J.-P. Bouchaud and E. Pitard, Anomalous dynamical light scattering in soft glassy gels, *Eur. Phys. J. E* **6**, 231 (2001).
- [34] L. Cipelletti, L. Ramos, S. Manley, E. Pitard, D. A. Weitz, E. E. Pashkovski, and M. Johansson, Universal non-diffusive slow dynamics in aging soft matter, *Faraday Discuss.* **123**, 237 (2003).
- [35] A. Mesaros, K. Fujita, H. Eisaki, S. Uchida, J. C. Davis, S. Sachdev, J. Zaanen, M. J. Lawler, and E.-A. Kim, Topological defects coupling smectic modulations to intra-unit-cell nematicity in cuprates, *Science* **333**, 426 (2011).
- [36] S. Wandel, F. Boschini, E. H. da Silva Neto, L. Shen, M. X. Na, S. Zohar, Y. Wang, S. B. Welch, M. H. Seaberg, J. D. Koralek, G. L. Dakovski, W. Hettel, M.-F. Lin, S. P. Moeller, W. F. Schlotter, A. H. Reid, M. P. Minitti, T. Boyle, F. He, R. Sutarto *et al.*, Enhanced charge density wave coherence in a light-quenched, high-temperature superconductor, *Science* **376**, 860 (2022).
- [37] H. Miao, J. Lorenzana, G. Seibold, Y. Y. Peng, A. Amorese, F. Yakhou-Harris, K. Kummer, N. B. Brookes, R. M. Konik, V. Thampy, G. D. Gu, G. Ghiringhelli, L. Braicovich, and M. P. M. Dean, High-temperature charge density wave correlations in $\text{La}_{1.875}\text{Ba}_{0.125}\text{CuO}_4$ without spin-charge locking, *Proc. Natl. Acad. Sci. USA* **114**, 12430 (2017).
- [38] S. C. Moss, K. Forster, J. D. Axe, H. You, D. Hohlwein, D. E. Cox, P. H. Hor, R. L. Meng, and C. W. Chu, High-resolution synchrotron x-ray study of the structure of $\text{La}_{1.8}\text{Ba}_{0.2}\text{CuO}_{4-y}$, *Phys. Rev. B* **35**, 7195 (1987).
- [39] A. N. Morozovska, E. A. Eliseev, V. Gopalan, and L.-Q. Chen, Landau-Ginzburg theory of charge density wave formation accompanying lattice and electronic long-range ordering, *Phys. Rev. B* **107**, 174104 (2023).
- [40] K. Yamada, C. H. Lee, K. Kurahashi, J. Wada, S. Wakimoto, S. Ueki, H. Kimura, Y. Endoh, S. Hosoya, G. Shirane, R. J. Birgeneau, M. Greven, M. A. Kastner, and Y. J. Kim, Doping dependence of the spatially modulated dynamical spin correlations and the superconducting-transition temperature in $\text{La}_{2-x}\text{Sr}_x\text{CuO}_4$, *Phys. Rev. B* **57**, 6165 (1998).
- [41] Z. Evenson, B. Ruta, S. Hechler, M. Stolpe, E. Pineda, I. Gallino, and R. Busch, X-ray photon correlation spectroscopy reveals intermittent aging dynamics in a metallic glass, *Phys. Rev. Lett.* **115**, 175701 (2015).
- [42] F. Perakis, K. Amann-Winkel, F. Lehmkuhler, M. Sprung, D. Mariedahl, J. A. Sellberg, H. Pathak, A. Sp ah, F. Cavalca, D. Schlesinger, A. Ricci, A. Jain, B. Massani, F. Aubree, C. J. Benmore, T. Loerting, G. Gr ubel, L. G. M. Pettersson, and A. Nilsson, Diffusive dynamics during the high-to-low density transition in amorphous ice, *Proc. Natl. Acad. Sci. USA* **114**, 8193 (2017).
- [43] Y. Horibe, Y. Inoue, and Y. Koyama, Direct observation of dynamic local structure in $\text{La}_{2-x}\text{Sr}_x\text{CuO}_4$ around $x = 0.12$, *Phys. Rev. B* **61**, 11922 (2000).